

## Prediction models for compressive strength of concrete with Alkali-activated binders

Arkamitra Kar<sup>\*1</sup>, Indrajit Ray<sup>2a</sup>, Avinash Unnikrishnan<sup>3b</sup> and Udaya B. Halabe<sup>4a</sup>

<sup>1</sup>Department of Civil Engineering, Birla Institute of Technology and Science-Pilani, Hyderabad - 500078, Telangana, India

<sup>2</sup>Department of Civil and Environmental Engineering, Faculty of Engineering, The University of the West Indies, St Augustine, Trinidad and Tobago

<sup>3</sup>Department of Civil and Environmental Engineering, Portland State University, Portland, OR 97201, USA

<sup>4</sup>Department of Civil and Environmental Engineering, West Virginia University, Morgantown, WV 26506, USA

(Received August 4, 2015, Revised December 11, 2015, Accepted February 2, 2016)

**Abstract.** Alkali-activated binder (AAB) is increasingly being considered as an eco-friendly and sustainable alternative to portland cement (PC). The present study evaluates 30 different AAB mixtures containing fly ash and/or slag activated by sodium hydroxide and sodium silicate by correlating their properties from micro to specimen level using regression. A model is developed to predict compressive strength of AAB as a function of volume fractions of microstructural phases (physicochemical properties) and ultrasonic pulse velocity (elastic properties and density). The predicted models are ranked and then compared with the experimental data. The correlations were found to be quite reasonable ( $R^2 = 0.89$ ) for all the mixtures tested and can be used to estimate the compressive strengths for similar AAB mixtures.

**Keywords:** alkali-activated binder; compressive strength; prediction model

### 1. Introduction

The manufacturing of portland cement (PC), the main binder of concrete, generates large amount of CO<sub>2</sub> (a greenhouse gas), cement kiln dust (solid waste), and consumes significant amount of heat energy. For that reason, alkali-activated binder (AAB) is increasingly being considered as an environmentally friendly or green alternative to PC. The AAB is produced by alkali activation of aluminosilicate compounds, with or without calcium ions, in the temperature range of 60° C to 90° C (Provis and van Deventer 2009). Since most of the aluminosilicate sources are waste or by-products, the AAB is regarded as sustainable and green construction material with great potential for use in civil infrastructures. Previous researches on AAB concretes primarily focused on the development of materials using limited number of aluminosilicates or calcium-based compounds and qualitative evaluations of their microstructural properties and strengths

---

\*Corresponding author, Assistant Professor, E-mail: [arkamitra.kar@hyderabad.bits-pilani.ac.in](mailto:arkamitra.kar@hyderabad.bits-pilani.ac.in)

<sup>a</sup>Professor

<sup>b</sup>Associate Professor

(Davidovits 1991, Davidovits 1994, Rees *et al.* 2004, Shi *et al.* 2006, Provis and van Deventer 2009). However, no systematic studies have been conducted on characterizing concrete with AAB consisting of different proportions of fly ash and slag cured at relatively lower temperature and correlating their properties from micro to specimen level. In 1981, inorganic polymeric materials were produced by mixing alkalis with burnt mixture of kaolinite, limestone and dolomite (Davidovits 1982). The binders were known as “geopolymer” since they were originated by inorganic poly-condensation, or “geo-polymerization” (Davidovits 1982, Davidovits 1994). This process is also known as alkali activation of aluminosilicate materials. During the past two decades, AAB have attracted strong interests all over the world due to their advantages of low energy cost, appreciable serviceability, and good durability compared to PC concrete (Shi *et al.* 2006, Smith and Comrie 1988, Davidovits 1991). A major incentive for further development of such AAB is created by the annual output of fly ashes from power plants and other by-product materials, such as slag, which is so enormous that there is a constant need to find new uses for them. Literature review (Van Jaarsveld 2000, Rees *et al.* 2004, Barbosa *et al.* 2000, Lee and van Deventer 2002) shows that x-ray diffraction (XRD) revealed limited information due to the substantial amorphous nature of AAB microstructure. Several researchers have conducted studies on the microstructural aspects of AAB using scanning electron microscopy (SEM) and energy dispersive x-ray (EDS), x-ray diffraction (XRD), and Fourier Transform Infrared Spectroscopy (FTIR) (Van Jaarsveld 2000, Rees *et al.* 2004, Barbosa *et al.* 2000, Lee and van Deventer 2002); However, their primary focus was to understand the underlying mechanisms of reactions and morphology of this complex system. No systematic studies of the wide range of AAB mixtures quantifying the volume fractions from the microanalysis and volume stoichiometry of the reaction products of varied AAB products were reported. Limited researches have been conducted to understand the interactions of alkali-activated binder pastes from the fly ash and calcium-silicate-hydrate paste from slag (van Deventer *et al.* 2010, Quillin *et al.* 2011). Durability of these AAB systems has also formed a prominent aspect of recent research (Shaikh 2014, Zahira and Aissa 2015). The present research addresses the limitations mentioned above by first understanding the AAB, fly ash, and slag interactions, and then estimating their volume fractions using combined microanalysis and regression techniques. The research methodology in this paper had undertaken the following steps: (i) Identified the chemistry of polymerization, (ii) Studied the effect of pre-blending of the starting materials, (iii) Obtained the optimum combination of fly ash and slag with activating solution and also identified the mixture which provides the best compressive strength, and (iv) Developed a combined microanalysis and regression technique to quantify the volume fractions of the different products of alkali activation of fly ash and slag. The volume fraction was estimated for ten mixtures containing different percentages of fly ash and slag, cured at three different temperatures using combined microanalysis and regression technique. This ultimately helps to estimate the paste volumes of various unknown AAB mixtures produced from different sources of fly ash and slag (Kar *et al.* 2014). The knowledge of the quantities of the microstructural phase volumes of the reacted AAB paste have been used in this study to develop a compressive strength prediction model for concrete with AAB at specimen level by correlating microscale characteristics with specimen level properties through regression. It was observed that the compressive strength of hardened AAB pastes at microscale followed the same trend as the compressive strength of concrete with AAB at specimen level. Also, positive correlation was observed between the microscale phase volume fractions and the compressive strength at both micro and specimen levels.

In a previous study, the present authors developed a combined microanalysis and regression

Table 1 Properties of the materials used in this study

Materials	Slag <sup>a</sup>	Fly Ash
Specific gravity	2.88	2.18
Specific surface(m <sup>2</sup> /kg)	580 (Blaine)	490 (Blaine)
Loss on ignition, %	0.06	3.00
SiO <sub>2</sub> , %	36.0	49.34
Al <sub>2</sub> O <sub>3</sub> , %	12.0	22.73
CaO, %	42.0	3.09
MgO, %	6.0	1.06
SO <sub>3</sub> , %	0.2	0.97
Na <sub>2</sub> O + 0.685 K <sub>2</sub> O, %	0.74	2.75
Fe <sub>2</sub> O <sub>3</sub> , %	1.8	16.01
Others, %	1.2	1.05

<sup>a</sup>The pH value (in water) for the slag is in the range of 10.5 ~ 12.7.

technique to quantify the volume fractions of the different products of alkali activation of fly ash and slag at the microstructural level (Kar *et al.* 2014). In a separate study by the present authors determined the ultrasonic pulse velocities (UPV) of concrete with AAB at specimen level (Kar *et al.* 2013) and observed that the compressive strength of concrete with AAB had a positive correlation with the UPV. Hence, compressive strength of concrete with AAB at specimen level was expressed as a function of the UPV and that concept has been used in the present study. The current study focuses on expressing the compressive strength as a function of the volume of microstructural phases (to represent the microscale parameter for compressive strength) and the UPV results (to represent the specimen level parameter for compressive strength). For this purpose, two major aspects were considered: (i) The mechanisms involved in AAB chemistry have not been fully decoded yet and it was assumed that correlation between the compressive strength and the microscale phase volumes could be linear or nonlinear. To overcome this issue, the present study adopts a multi-variate regression model with a several linear and nonlinear specification. (ii) The present study involved mixture proportions where fly ash was partially replaced by slag. The chemistry of the polymerization of fly ash involves alkali activation, whereas, the chemistry of slag hydration resembles PC hydration at a much lower rate. So, combination of these two phenomena was considered while developing the model to predict the compressive strength of concrete with AAB in this study.

## 2. Materials and experimental methods

### 2.1 Materials

The following materials were used in this study

- Fly ash: Class F fly ash conforming to ASTM C618 (Standard Specification for Coal Fly Ash and Raw or Calcined Natural Pozzolan for use in Concrete) obtained from a local coal power plant. The specific gravity, specific surface area and oxide composition are listed in Table 1.

- Slag: Ground granulated blast furnace slag or slag conforming to Grade 100 of ASTM C989 (Standard Specification for Slag Cement for Use in Concrete and Mortars) obtained from local steel plant.
- Coarse aggregate: 12.5 mm (½ in.) graded and crushed limestone conforming to ASTM C33/C33M-13 (Standard Specification for Concrete Aggregates). The saturated surface dry (SSD) bulk specific gravity was 2.68.
- Sand: Locally available 4.75 mm (0.187 in.) graded river sand conforming to ASTM C33/C33M-13. The fineness modulus and the SSD bulk specific gravity of sand were 2.79 and 2.59, respectively.
- Admixture: Commercially available high-range water reducing admixture (HRWRA), conforming to ASTM C494 Type F (Specification for Chemical Admixtures for Concrete).

## 2.2 Mix proportions and mixing procedure

### 2.2.1 Selection of mix proportions

The mix proportions were selected in order to compare their influences on the microstructural properties of the cementitious systems for different combinations of fly ash with slag replacement, at different ages, and different temperatures. The starting materials can be categorized into two groups - unreacted aluminosilicate and activating solution. As the aluminosilicates are primarily composed of industrial by-products, they will lead to lots of uncertainties in the characteristics of the finished product. Moreover, the activating solution reacts with the aluminosilicates through a polymerization mechanism, whose chemistry is yet to be fully decoded. This polymerization process governs the development of strength of the building material and it is dependent on several

Table 2 Final concrete mix proportions for Alkali activated fly ash and/or slag (Ms modulus = 1.4)

Aluminosilicate	Mixture Name	Fly ash	Slag
		Kg/m <sup>3</sup>	Kg/m <sup>3</sup>
100 % Fly ash	FA 100	400	0
85% Fly ash + 15% slag	FA 85 SG 15	340	60
70% Fly ash + 30% slag	FA 70 SG 30	280	120
50% Fly ash + 50% slag	FA 50 SG 50	200	200
30% Fly ash + 70% slag	FA 30 SG 70	120	280
15% Fly ash + 85% slag	FA 15 SG 85	60	340
100% slag	SG 100	0	400
Pre blend 100% fly ash and solid NaOH for 15 days	FA 100 p15	400	0
Pre blend 100% fly ash and solid NaOH for 30 days	FA 100 p30	400	0
Pre blend 100% fly ash and solid NaOH for 60 days	FA 100 p60	400	0

Note: The quantity of coarse aggregate was kept constant at 1209 kg/m<sup>3</sup> and that of fine aggregate at 651 kg/m<sup>3</sup> for all mixtures. Quantity of Sodium silicate (liquid) was 129.43 kg/m<sup>3</sup> and that of sodium hydroxide (solid) was 10.57 kg/m<sup>3</sup> for all mixtures. The quantity of HRWRA used was in the range of 5060 ~ 6745 ml/m<sup>3</sup>.

factors - (i) the ratio of  $\text{SiO}_2/\text{Na}_2\text{O}$  in the activating silicate solution (2:1 in this case) , (ii) the ratio of  $\text{SiO}_2/\text{Na}_2\text{O}$  in the activating solution (also known as Ms ratio or Ms modulus), (iii) the ratio of  $\text{SiO}_2/\text{Al}_2\text{O}_3$  in the aluminosilicate (2.1 in this case), (iv) the ratio of water-to-AAB solids (w/s) (0.20 in this case), and (v) the curing temperature, i.e., the temperature at which the polymerization is allowed to occur. The mixture proportions used in the present study have been furnished in detail in Kar *et al.* (2013). They are summarized in Table 2. For initial assessment to estimate the best Ms modulus, the compressive strengths of 2 in. cube specimens were measured for different AAB mixtures as shown in Table 2. It was observed that Ms modulus of 1.4 resulted in the best compressive strengths at all ages and the strengths increased with curing temperature. A total of 10 mixtures were produced at each of three different temperatures – 23°C, 40°C, and 60°C using different combinations of fly ash, and slag. Thus a total of 30 different mixtures were used for the present study.

### 2.2.2 Mixing procedure

The dry raw materials were blended to obtain a uniform mixture. Sand, limestone and fly ash and/or slag or both were mixed thoroughly to ensure uniformity of concrete specimens. Water, sodium silicate and sodium hydroxide were mixed separately in proper proportions to obtain a uniform blend. The addition of water to sodium hydroxide generates significant amount of heat; hence, the mixture was allowed to stand for 24 hours at room temperature to ensure full dissipation of any additional heat and consequent temperature variation which would otherwise influence the polymerization reaction of alkali-activate aluminosilicates. The liquid blend was then added to the solid mix. As the AAB tends to set very rapidly, small quantity of concrete was batched at a time. For this reason, hand mixing was preferred over machine mixing. The liquid and solid mixtures were combined very carefully, to avoid any kind of chemical burn due to the corrosive nature of the sodium hydroxide. The mix was prepared and placed in the molds very rapidly to complete the casting process at desirable workability. After casting, the molds were left undisturbed for 24 hours at constant temperature and humidity, under moist condition. Then the specimens were subjected to three different temperature-curing as mentioned in 2.2.1.

## 2.3 Experimental program

In this study, scanning electron microscopy (SEM) and energy dispersive x-ray spectroscopy (EDS) and degree of reaction tests were conducted for quantitative identification of the microstructural characteristics of AAB binders. X-ray diffraction (XRD) and Fourier transform infrared (FTIR) spectroscopy techniques were implemented to qualitatively understand the underlying mechanism of the reactions of various alkali-activated binders and their nature of products.

### 2.3.1 Microanalysis techniques

Powder XRD was performed on all samples using a Bruker D8 Discover X-ray Diffractometer. The  $\text{CuK}\alpha$  X-rays were generated at 40 mA and 40 kV. FTIR spectra were obtained using a PerkinElmer Spectrum 100 FTIR spectrometer with Universal Attenuated Total Reflectance ATR accessory, in absorbance mode, within the frequency range of 4000 - 400 $\text{cm}^{-1}$ . As mentioned previously, the present study requires knowledge about the quantity of the different phases in the microstructure of the polymer product. Thus SEM-EDS techniques were used for further quantification of the phases which were confirmed to be present in the AAB microstructure

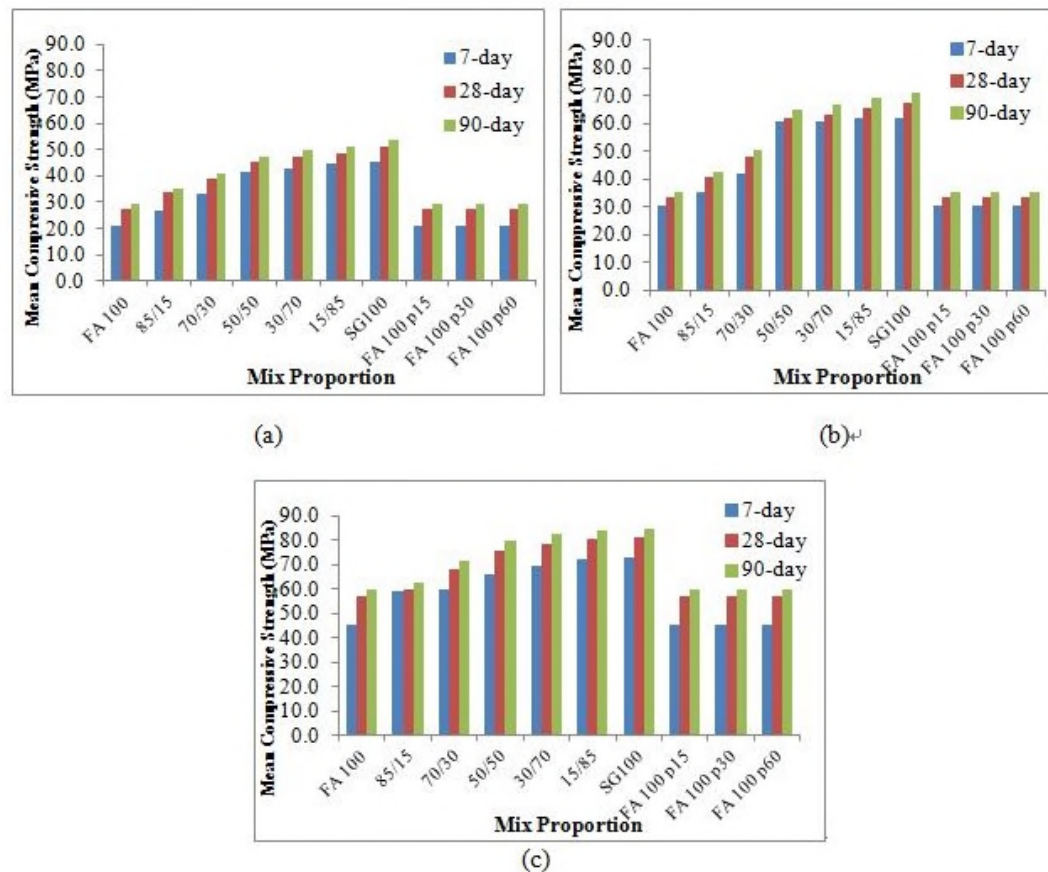


Fig. 1 Compressive strength data for all mixtures at different ages at different temperatures (a) 23°C, (b) 40°C, and (c) 60°C.

Note: Please keep this as color figure

through the XRD and FTIR studies. A state-of-the-art thermal Field Emission Scanning Electron Microscope (FE-SEM), JSM-7600F (accompanied by an EDS analyzer), supplied by JEOL Limited was used for the imaging process. One of the major factors that govern the progress of polymerization is the curing temperature. Hence, it is of utmost importance to have knowledge of the influence of the curing temperature on the degree of reaction. The technique suggested by Fernandez-Jimenez *et al.* (2006) was followed to determine the degree of reaction at different temperatures, and thus determine the effect of curing temperature on the degree of reaction, as described in detail in Kar *et al.* (2013).

## 2.4 Specimen level testing

### 2.4.1 Test for compressive strength

Compressive strengths of 101.6 mm diameter and 203.2 mm long cylinder specimens were measured in accordance with ASTM C39 (Standard Test Method for Compressive Strength of Cylindrical Concrete Specimens). Tests were conducted at 7, 28, and 90 days after casting. Both

Table 3 Ultrasonic pulse velocity results at different ages for all AAB specimens

Mix	Age (Days)	Ultrasonic pulse velocity (Km/s)		
		23°C	40°C	60°C
FA 100	7	4.04	4.33	4.69
	28	4.33	4.63	5.21
	90	4.37	4.64	5.28
FA 85 SG 15	7	4.31	4.64	5.42
	28	4.65	4.65	5.51
	90	4.71	4.69	5.54
FA 70 SG 30	7	4.63	4.64	5.69
	28	4.94	4.65	5.70
	90	5.23	4.92	5.82
FA 50 SG 50	7	5.53	5.51	5.89
	28	5.71	5.55	5.90
	90	5.80	5.59	6.05
FA 30 SG 70	7	5.62	5.68	6.12
	28	5.82	5.74	6.13
	90	5.85	5.80	6.26
FA 15 SG 85	7	5.75	5.75	6.32
	28	5.83	5.85	6.34
	90	5.88	5.87	6.36
SG 100	7	5.98	5.85	6.32
	28	6.03	5.90	6.38
	90	6.08	5.93	6.39
FA 100 p15	7	4.04	4.33	4.69
	28	4.33	4.63	5.21
	90	4.37	4.64	5.28
FA 100 p30	7	4.04	4.33	4.69
	28	4.33	4.63	5.21
	90	4.37	4.64	5.28
FA 100 p60	7	4.04	4.33	4.69
	28	4.33	4.63	5.21
	90	4.37	4.64	5.28

curing time and curing temperature influence the compressive strength of AAB concrete specimens. The specimens were cured after 24 hours of casting. Three different temperatures, i.e., 23°C (room temperature), 40°C, and 60°C (the last two temperatures were obtained in an oven) were used to cure the respective specimens for 24 hours. The average values of compressive strength of three specimens for each mixture proportion were used for the present study. The results for the compressive strength tests are presented in Fig. 1.

#### 2.4.2 Ultrasonic pulse velocity test

The ultrasonic pulse velocity (UPV) test has been long established as an efficient nondestructive test method to determine the velocity of longitudinal (compressional) waves. The UPV test consists of measuring the time taken by a pulse - leading to the name of the technique - to travel a measured distance. The apparatus includes transducers which are kept in contact with

concrete, a pulse generator with a frequency in the range of 10 to 150 kHz, an amplifier, a time measuring circuit, and a digital display of the time taken by the pulse of longitudinal waves to travel between the transducers through the concrete. The test method follows the guidelines prescribed by ASTM C597-09 (C597-09 Standard Test Method for Pulse Velocity Through Concrete). The ultrasonic pulse velocities were obtained from tests on 75 mm × 75 mm × 275 mm (width × depth × length) prisms. The results for the compressive strength tests are presented in Table 3.

### 3. Formulation of proposed regression model

Attempts have been made in the past to formulate a suitable mathematical model to predict the compressive strength of concrete, particularly PC concrete, at various ages with satisfactory accuracy. De Larrard (1999) and De Larrard and Belloc (1997) proposed a comprehensive model for predicting the concrete compressive strength on the basis of the mixture composition and accounting for the physical and chemical characteristics of the concrete mixture, such as cement type and degree of hydration and proportions of aggregates and cement. Other researchers (Abd *et al.* 2008 (Liu *et al.* 2009, Huang *et al.* 2011) investigated the relationship between clinker phase composition and strength after a certain hydration period using multiple linear regression analysis and thus assuming an additive action of the phases involved. In a recent study, the present authors (Kar *et al.* 2013) established an equation to determine the volume of the reaction products due to the alkali activation of the fly ash and slag. Hence, those volumes were used as input parameters for the model proposed by this study instead of the initial composition of the raw materials. According to existing research, rapid determination or prediction of the strength of concrete could be obtained by: (i) suitable prediction model which considers the microstructural properties of the AAB, and (ii) accelerated strength testing results. Some existing compressive strength prediction models for PC concrete combined these two aspects (Abd *et al.* 2008, Liu *et al.* 2009, Huang *et al.* 2011). In one such case, the accelerated strength test results were obtained indirectly through nondestructive testing, such as rebound hammer test (Liu *et al.* 2009, Huang *et al.* 2011) or ultrasonic pulse velocity tests (Abd *et al.* 2008, Huang *et al.* 2011). The basic concept of the model was to produce a reliable relationship between compressive strength of concrete and its own characteristics at the microstructural level as well as the specimen level. Due to the uncertainties associated with the microstructure of concrete, the models must be formulated using some experimental results (Abd *et al.* 2008). Kar *et al.* 2014 found that the compressive strengths of the hardened AAB cubes and those of the AAB concrete cylinders showed similar trends. This is true in case of each of the three different curing temperatures as well as in case of different percentages of slag being used here to replace fly ash. Hence it was understood that the microstructural properties of the AAB definitely influenced the characteristics of the AAB concrete specimens.

In another study, Kar *et al.* (2013) found that the compressive strengths of concrete with AAB showed positive correlations with the ultrasonic pulse velocities at the specimen level. Hence, the ultrasonic pulse velocity was also included as an input parameter along with the microstructural phase volumes in the proposed model to predict the compressive strength of concrete with AAB.

In the conventional material modeling process, regression analysis is an important tool for constructing a model (Liu *et al.* 2009). For the purpose of the present study, all the above findings and suggestions were kept in mind while developing a model to correlate the microstructural properties with the specimen level properties. The concept of quantitative determination of the

different phases in the AAB microstructure was combined with the results from the ultrasonic pulse velocity test in order to come up with a multi-variable regression model for AAB concrete. Linear and several nonlinear regression models were tested due to the uncertainties of the chemistry of the microstructural reactions because of which we were unsure of the nature of the relationship of compressive strength with microstructural phase volumes. The proposed regression model can be expressed as

$$f_c' = \text{nlf}(v_{f,AAB}, v_{f,CSH(S)}, v) \quad (1)$$

where  $f_c'$  is the AAB compressive strength;

nlf denotes nonlinear function;

$v_{f,AAB}$  = volume fraction of reacted AAB paste products at any given degree of reaction

$v_{f,CSH(S)}$  = volume fraction of CSH(S) at degree of slag hydration,  $\alpha$  (microstructural properties);

$v$  denotes the results obtained from the ultrasonic pulse velocity test at the specimen level.

Modifying Eq. (1), the proposed equation is of the form

$$f_c' = a(v_{f,AAB})^b + c(v_{f,CSH(S)})^d + e(v)^f + k + \varepsilon \quad (2)$$

where  $a$  and  $b$  are obtained from the regression to denote the effect of  $v_{f,AAB}$  ;

$c$  and  $d$  are obtained from the regression to denote the effect of  $v_{f,CSH(S)}$  ;

$e$  and  $f$  are obtained from the regression to denote the effect of the ultrasonic pulse velocity; and

$k$  denotes the effect of all other uncertainties in the study ;

$\varepsilon$  denotes the error term which is normally distributed with zero mean and constant variance.

Note that the linear regression is a special case of the nonlinear specification described in Eqs. (1) and (2). The volume fractions were determined using the technique described in Kar *et al.* (2014). The ultrasonic pulse velocities were determined experimentally using the procedure described in Kar *et al.* (2013). The statistical analyses were performed using the software 'R'. Instead of selecting an arbitrary empirical equation to represent the compressive strength model, the present study referred to the equations suggested by previous researchers (Huang *et al.* 2011). Several multi-variable regression models have been previously developed and published in various refereed journals and conference proceedings (Wiebenga 1968, Bellander 1979, Tanigawa *et al.* 1984, Sriravindrajah 1988, Arioglu and Manzak 1991, Ramyar and Kol 1996, Hobbs and Kebir 2007, Huang *et al.* 2011, Panzera *et al.* 2011). To be statistically unbiased in selection and application, the models suggested by previous researchers (Wiebenga 1968, Bellander 1979, Tanigawa *et al.* 1984, Sriravindrajah 1988, Arioglu and Manzak 1991, Ramyar and Kol 1996, Hobbs and Kebir 2007, Huang *et al.* 2011, Panzera *et al.* 2011) were modified to satisfy the requirements of the present study. The models were formulated using 60 out of a total of 90 experimental data points as calibration data. The remaining 30 data points were then used to test the accuracy and the validation of the proposed model.

For each model form, the independent variables or regressors were the volume fractions of the AAB reaction product and the CSH(S) due to slag hydration (both dimensionless quantities), along with the ultrasonic pulse velocity (in km/s). The independent variable or regressed was the compressive strength (in MPa). Table 4 gives the model forms which were obtained as outputs from R. Table 4 also presents the mean square error (MSE) due to each model and the corresponding ranks assigned to each model, using the MSE as a measure of accuracy to select the most suitable model for the purpose of the present study. In the next section, the selection of the most suitable model for this study is discussed in detail.

Table 4 Different models for  $f_c'$  in Terms of  $v_{f,AAB}$ ,  $v_{f,CSH(S)}$  and  $v$ 

Model No.	With constant	Mean Square Error	Rank
1	$f_c' = -4.535v_{f,AAB} + 13.852v_{f,CSH(S)} + 18.264v - 55.323$	0.053	1
2	$f_c' = 0.899v_{f,AAB}^3 + 38.861v_{f,CSH(S)}^3 + 18.979v - 57.001$	0.128	2
3	$f_c' = 39.893v_{f,AAB} + 87.858v_{f,CSH(S)} - 0.0013v^4 + 28.093$	0.886	4
4	$f_c' = -8.808v_{f,AAB} + 10.746v_{f,CSH(S)} - 89.740v + 10.135v^2 + 223.932$	0.910	5
5	$\ln(f_c') = 0.1660v_{f,AAB} + 0.2621v_{f,CSH(S)} + 2.1694\ln(v) + 0.0583$	1806.167	9
6	$\ln(f_c') = 0.0134\ln(v_{f,AAB}) - 0.0025\ln(v_{f,CSH(S)}) + 2.3219\ln(v) - 0.1024$	1797.345	7
7	$\ln(f_c') = 0.4253(\sqrt{\ln((v_{f,AAB} + v_{f,CSH(S)})^3(v^4))}) + 3.0873$	1797.345	7
8	$\sqrt{f_c'} = -0.4385/v_{f,AAB} - 0.5091/v_{f,CSH(S)} + 0.0861v(1/v_{f,AAB} + 1/v_{f,CSH(S)}) + 7.0568$	1522.051	6
9	$f_c' = 40.45v_{f,AAB} + 88.38v_{f,CSH(S)} + 26.63$	0.846	3

Table 5 Output from R for proposed model

Formula: $f_c' \sim (a * v_{f,AAB} + c * v_{f,CSH} + e * v + k)$				
Parameters:	Estimate	Std. Error	t value	Pr(> t )
a	-4.535	7.099	0.639	0.5255
c	13.852	7.767	1.783	0.0799
e	18.264	1.282	14.242	<2E-16
k	-55.323	6.232	-8.877	2.85E-12

#### 4. Selection of suitable prediction model

The models were ranked based on their respective mean square errors obtained over 30 validation data points. Model with the least MSE was assigned as rank 1 and rankings increased with increasing MSE (Table 4). The Model 1 as shown in equation 3 had the best performance.

$$f_c' = -4.535 v_{f,AAB} + 13.852 v_{f,CSH(S)} + 18.264v - 55.323 \quad (3)$$

While specifying any regression model it is necessary to analyze whether all the independent variables are statistically significant or not. Hence, the output from R was analyzed to determine the statistical significance of the variables. The  $p$ -values of the model parameters provided an indication of the most significant parameters influencing the compressive strength. The outputs of the regression coefficients for the proposed model have been presented in Table 5.

From Table 5, it can be shown that all the independent variables considered in this work were found to be significant at 10% significance level. The AAB is a complex material and the proposed equation combines both microstructural phases (physicochemical properties) as well as UPV parameter (elastic/density properties); therefore the 10% significance level seems reasonable.

Fig. 2 shows the comparison between the predicted compressive strengths and the experimental values of set of data to test the accuracy of Model 1. It shows a very good agreement with corresponding  $R^2$  value of 0.898. The Fig. 2 shows that the data points were scattered nearly evenly around the dotted line denoting the predicted compressive strengths, indicating that the predictions were almost unbiased. Thus, the accuracy of the model was assessed and established using an intuitive measure i.e. the mean square error as well as the coefficient of regression,  $R^2$ , which corroborated the "goodness of fit". After establishing Model 1 as the most accurate model

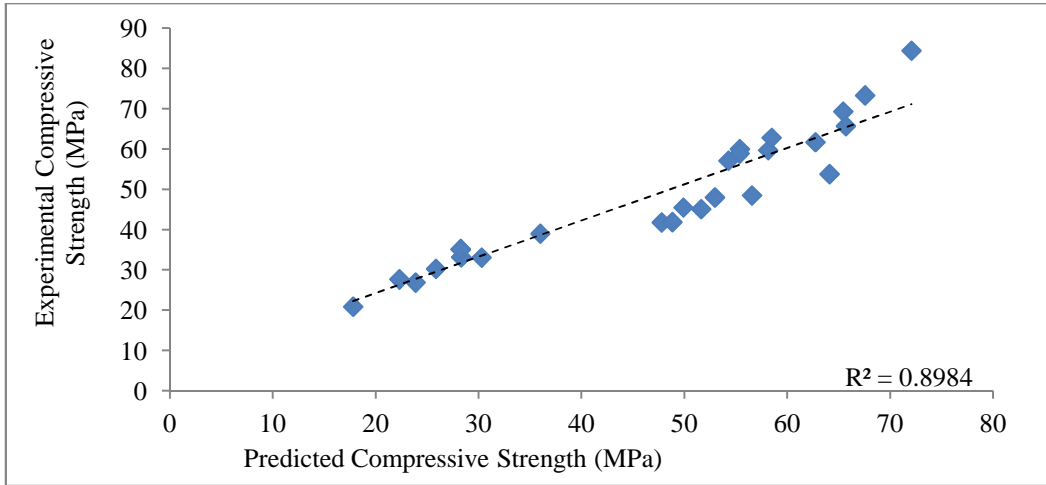
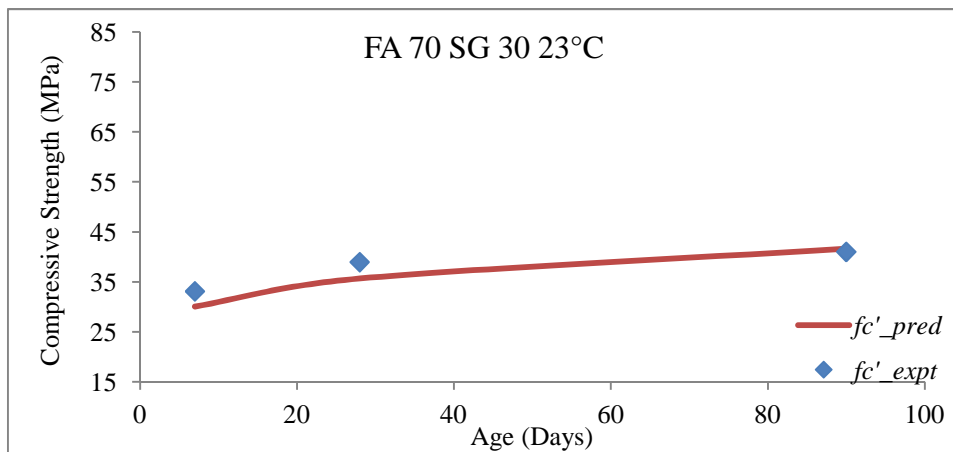
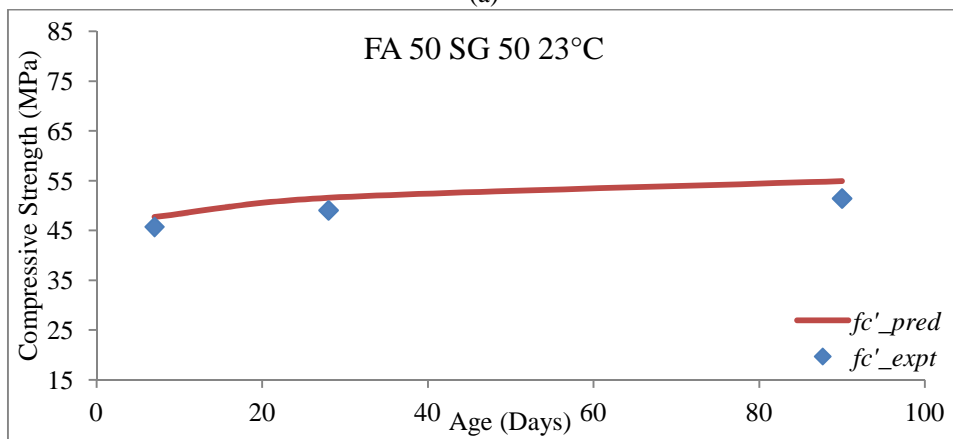


Fig. 2 Comparison between the predicted compressive strengths and the experimental values

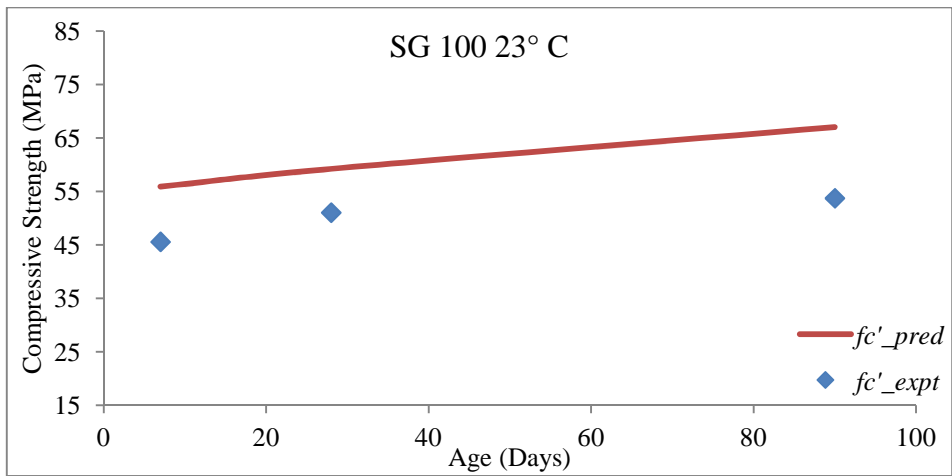


(a)

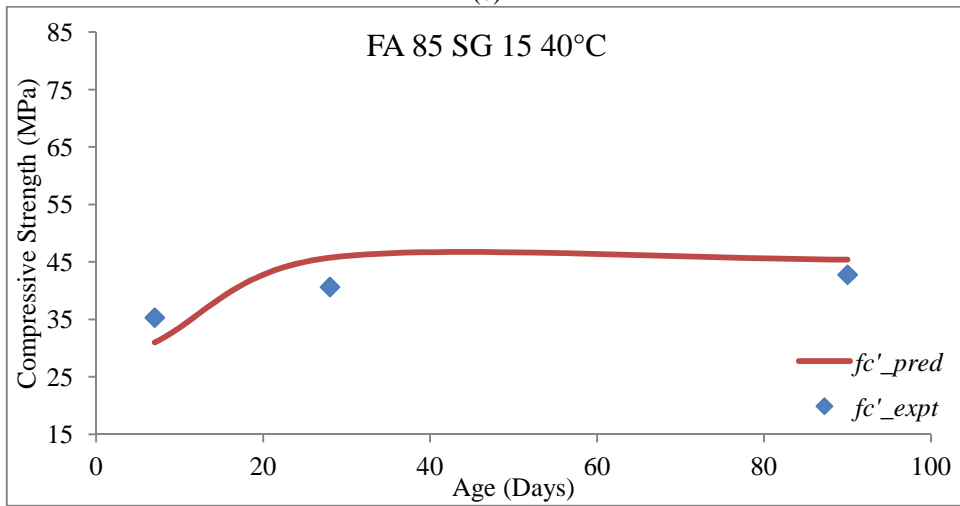


(b)

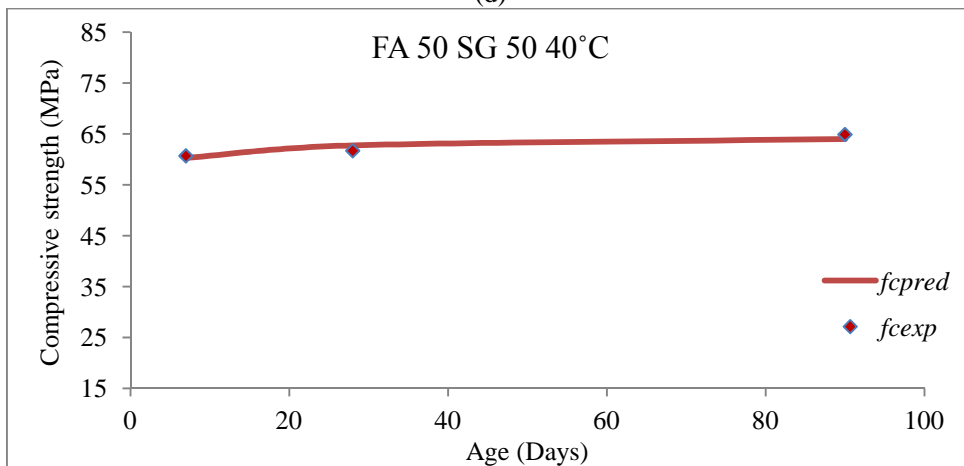
Fig. 3 Comparison between predicted and experimental compressive strengths for selected AAB concrete mixtures



(c)

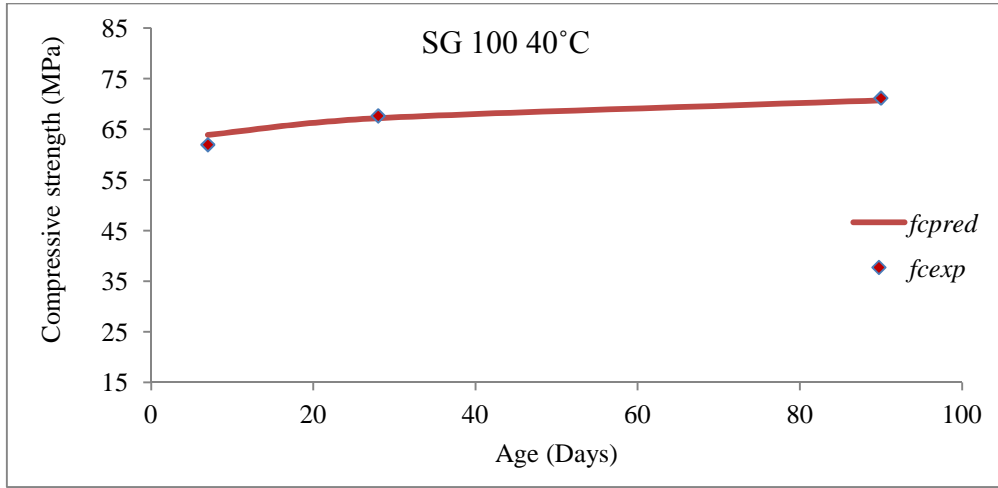


(d)

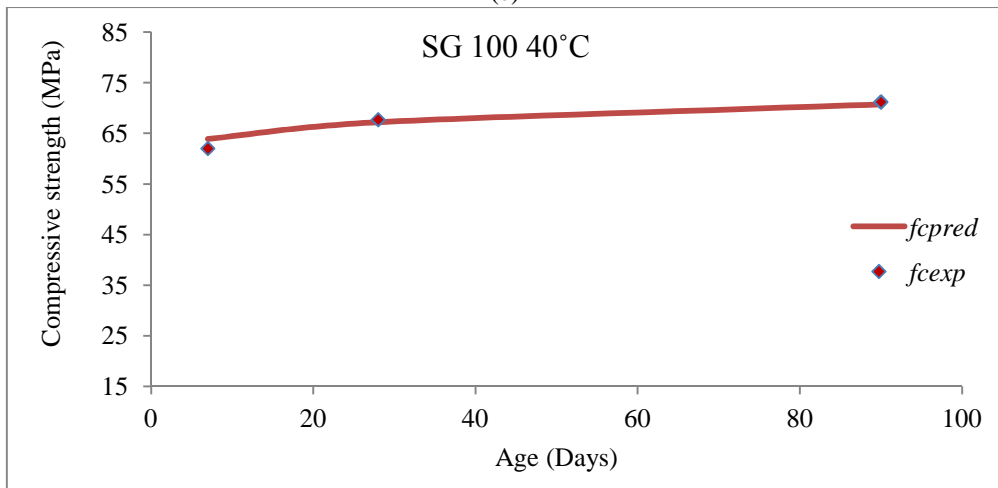


(e)

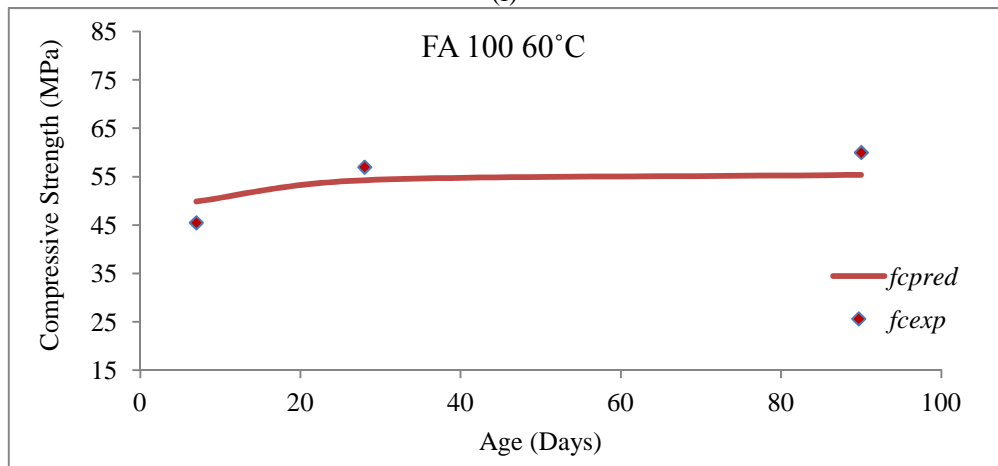
Fig. 3 Continued



(e)



(f)



(g)

Fig. 3 Continued

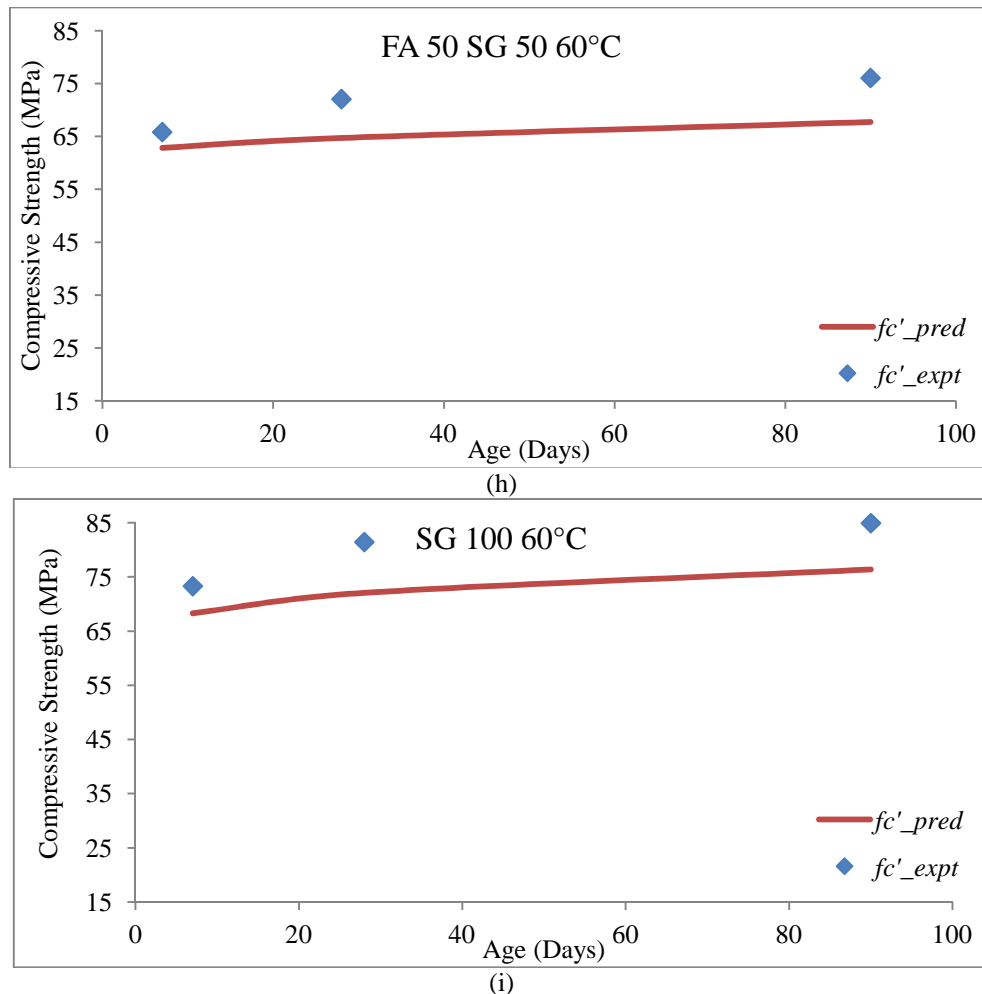


Fig. 3 Comparison between predicted and experimental compressive strengths for selected AAB concrete mixtures

for all mixtures in the present study, the next step was to test its accuracy in predicting the compressive strengths for individual mixtures. The Fig. 3 shows the outcomes of this test for individual mixture for selected mixtures from the study as furnished in section 5.

## 5. Comparison of the results of the proposed model with experimental data

Fig. 3(a) through (i) show the comparison of the predicted and experimental compressive strengths data of representative nine selected mixtures in the present study. All mixtures are not furnished here for brevity. The experimental and predicted values for the compressive strengths were found to be reasonably close to each other by inspection. No general trend of overestimation or underestimation can be inferred as the predicted line has been found to pass the experimental values both above and below them; and in both the cases the values were close. For mixtures not

shown in this graph, both the predicted lines and the experimental values were also reasonably close.

## 6. Conclusions

Based on the above study the following conclusions are made:

- A number of AAB mixtures containing fly ash and/or slag activated by alkalis are developed and measured for their compressive strengths and microstructural properties
- A model is developed to predict the compressive strength of such concretes as a function of ultrasonic pulse velocity and volume fractions of microstructural phases
- A regression model is developed between compressive strength and volume fraction of reacted AAB paste products at a certain degree of reaction, volume fraction of CSH(S) at degree of slag hydration, and microstructural properties
- Different models for compressive strength are ranked with respect to the values of mean square error (MSE) with the smallest values of MSE assigned as rank 1 and rankings increase with the increasing MSE
- The Model 1 (as shown in equation (3)) is selected as the best performing model for prediction of the compressive strength of AAB concrete as a function of the microstructural volume fractions and the ultrasonic pulse velocities at specimen level
- The predicted models are compared with the experimental data and the correlations were found to be quite reasonable for all the mixtures
- This model can set a guidelines for estimating compressive strength of various AAB from fundamental parameters such as volume fractions and ultrasonic pulse velocity
- In future, this model can be validated with the more field and real life data for different types of AAB concrete and the models can be revalidated with the additional information.

## Acknowledgements

Special thanks are due to the American Society of Civil Engineers (ASCE) for providing 2012 ASCE Freeman Fellowship to the first author in support of this research. The authors gratefully acknowledge Arrow concrete company for donating fly ash and slag and PQ Corporation for providing sodium silicate solutions used in this study. Special thanks to West Virginia University - Shared Research Facility for the SEM-EDS facility. The authors would also like to acknowledge the support of Dr. Ben Dawson-Andoh, (Professor, Wood Science and Technology, Division of Forestry and Natural Resources, West Virginia University) for his help with the degree of reaction measurements of AAB.

## References

- Abd, S.M., Mohd. Zain, M.F. and Abdul Hamid, R. (2008), "Modeling the prediction of compressive strength for cement and foam concrete", *International Conference of Construction and Building Technology (ICCBT 2008)*, Kuala Lumpur, Malaysia.
- Arioglu, E. and Manzak, O. (1991), "Application of 'SonReb' method to concrete samples produced in

- yedpa construction site,” *Prefabrication Union*, pp. 5-12. (in Turkish)
- Barbosa, V.F. and MacKenzie, K.J. (2003), “Synthesis and thermal behaviour of potassium sialate geopolymers”, *Mater. Lett.*, **57**(9), 1477-1482.
- Bellander, U. (1979), “NTD testing methods for estimating compressive strength in finished structures-evaluation of accuracy and testing system”, *RILEM Symposium Proceedings on Quality Control of Concrete Structures*, Session 2.1, Swedish Concrete Research Institute, Stockholm, Sweden, 37-45.
- Davidovits, J. (1982), “Mineral polymers and methods of making them”, US Patent 4,349,386
- Davidovits, J. (1991), “Geopolymers: Inorganic polymeric new materials”, *J. Therm. Anal.*, **37**(8), 1633-1656.
- Davidovits, J. (1994), “Geopolymers: Inorganic polymeric new materials”, *J. Mater. Edu.*, **16**, 91-139.
- De Larrard, F. (1999), *Concrete mixture proportioning: A Scientific Approach*, E&FN Spon, London.
- De Larrard, F. and Belloc, A. (1997), “The influence of aggregate on the compressive strength of normal and high-strength concrete”, *ACI Mater. J.*, **94**(5), 417-426.
- Fernandez-Jimenez, A., de la Torre, A.G., Palomo, A., Lopez-Olmo, G., Alonso, M.M., Aranda, M.A.G., (2006), “Quantitative determination of phases in the alkaline activation of fly ash. Part II: Degree of reaction”, *Fuel*, **85**(14), 1960-1969.
- Hobbs, B. and Kebir, M.T. (2007), “Non-destructive testing techniques for the forensic engineering investigation of reinforced concrete buildings”, *Forensic Sci. Int.*, **167**(2), 167-172.
- Huang, Q., Gardoni, P. and Hurlbaus, S. (2011), “Predicting concrete compressive strength using ultrasonic pulse velocity and rebound number”, *ACI Mater. J.*, **108**(4), 403-412.
- Kar, A., Halabe, U.B., Ray, I. and Unnikrishnan, A. (2013), “Nondestructive characterizations of Alkali activated fly ash and/or slag concrete”, *Eur. Sci. J.*, **9**(24), 52-74.
- Kar, A., Ray, I., Halabe, U.B., Unnikrishnan, A. and Dawson-Andoh, B. (2014), “Characterizations and estimation of Alkali activated binder paste from microstructures”, *Int. J. Concrete Struct. Mater.*, **8**(3), 213-228.
- Lee, W.K.W. and van Deventer, J.S.J. (2002), “Effects of anions on the formation of aluminosilicate gel in geopolymers”, *Ind. Eng. Chem. Res.*, **41**(18), 4550-4558.
- Liu, R., Wenshun, H. and Yonghon X. (2009), “Effect of crumb rubber on the mechanical properties of concrete”, *J. Build. Mater.*, **12**(3), 341-344.
- Panzer, T.H., Christoforo, A.L., Bowen, C.R., Cota, F.P. and Borges, P.H.R. (2011), *Ultrasonic pulse velocity evaluation of cementitious materials*, INTECH Open Access Publisher, September
- Provis, J.L. and van Deventer, J.S.J. (2009), *Geopolymers: structure, processing, properties and industrial applications*, Publisher: Oxford: Woodhead ; Boca Raton, FL : CRC Press.
- Ramyar, K. and Kol, P. (1996), “Destructive and non-destructive test methods for estimating the strength of concrete”, *Cement Concrete World* (in Turkish) (2), 46-54.
- Rees, C., Lukey, G.C. and Van Deventer, J.S.J. (2004), “The role of solid silicates on the formation of geopolymers derived from coal ash”, *Proceedings of the International Symposium of Research Students on Material Science and Engineering*, India, December.
- Shaikh, Faiz U.A. (2014), “Effects of alkali solutions on corrosion durability of geopolymer concrete”, *Adv. Concrete Constr.*, **2**(2), 109-123.
- Shi, C., Krivenko, P. and Roy, M. (2006), *Alkali-activated cements and concretes*, Taylor & Francis, London and New York.
- Smith, J.W. and Comrie, D.C. (1988), “Geopolymeric building materials in third world countries”, Davidovits, J., Orlinski, J. (Eds.), *Proceedings of the 1st Int. Conf. Geopolymer*, **88**, 89-92.
- Sriravindrajah, R., Loo, Y.H. and Tam, C.T. (1988), “Strength evaluation of recycled-aggregate concrete by in-situ tests”, *Mater. Struct.*, **21**(4), 289-295.
- Tanigawa, Y., Baba, K. and Mori, H. (1984), “Estimation of concrete strength by combined nondestructive testing method”, Special Publication, **82**, 57-76.
- Van Jaarsveld, J.G.S. (2000), “The physical and chemical characterisation of fly ash based geopolymers”, Ph.D. Thesis, Department of Chemical Engineering, University of Melbourne, Australia.
- Wiebenga, J.G. (1968), “A comparison between various combined non-destructive testing methods to derive

the compressive strength of concrete”, Report kB1-68-61/1418, Inst. TNO Veor Bouwmaterialen en Bouwconstructies, Delft, the Netherlands.  
Zahira, S.N. and Aissa, A. (2015), “Modeling the alkali aggregate reaction expansion in concrete”, *Comput. Concrete*, **16**(1), 37-48.

CC

